Link sito dell'editore: https://ieeexplore.ieee.org/xpl/RecentIssue.jsp?punumber=22

Link codice DOI: https://ieeexplore.ieee.org/document/7560593

Citazione bibliografica dell'articolo:

G. Monti, L. Corchia, L. Tarricone and M. Mongiardo, "A Network Approach for Wireless Resonant Energy Links Using Relay Resonators," in *IEEE Transactions on Microwave Theory and Techniques*, vol. 64, no. 10, pp. 3271-3279, Oct. 2016, doi: 10.1109/TMTT.2016.2601092.

A Network Approach for Wireless Resonant Energy Links Using Relay Resonators

Giuseppina Monti, *Senior Member, IEEE,* Laura Corchia, Luciano Tarricone, *Senior Member, IEEE,* Mauro Mongiardo, *Fellow, IEEE*

***Abstract*—In this paper a network approach for the analysis of a wireless resonant energy link consisting of N inductively coupled LC resonators is proposed. By using an artificial transmission line approach, the wireless link is modeled as a transmission line described by effective parameters. It is shown that the analyzed system exhibits a pass–band filter behavior. More specifically, the reported results demonstrate that in the wireless link pass–band the effective parameters assume negative values resulting in a negative phase delay. Useful design formulas are derived and validated by comparisons with experimental data.**

***Index Terms*—Wireless Energy Transfer, Wireless Power Transmission, Magnetic Coupling, Multi-hop Wireless Transmission, Resonators, Artificial Transmission Line.**

I. Introduction

Reactive Wireless Power Transfer (WPT) based on near field magnetic coupling, also referred to as Wireless Resonant Energy Link (WREL), is currently receiving considerable interest [1]–[12]. Generally, a WREL consists of one transmitter and one receiver; oftentimes, in order to extend the range of the transmitter, multi–hop schemes are adopted [13]–[18]. In these schemes, synchronous resonators (relay elements) are added between the transmitting and the receiving resonators. Naturally, by adding a considerable number of relay elements the presence of the magnetic field may extend significantly in space. So far, the study of multi-hop wireless inductive links has been done by considering each specific case.

For instance, in [13], a two-hop wireless link for capsule endoscopy inspection is presented: the proposed link exploits the use of a relay resonator embedded in the patient's jacket in order to enhance the power transfer efficiency between a resonator on the floor and a capsule endoscopy. Similarly, in [14] the case of a single relay is considered and a design approach able to guarantee an improvement of the energy efficiency with respect to a two-coil link is proposed. In [15], a detailed analysis of a system using one or two relay resonators is performed. The effect on the performance of the WPT link of the position of the repeaters is analyzed demonstrating that for optimum operation a frequency adjustment is necessary in the case where the repeater is placed in close proximity to the transmitter or to the receiver.

However, when many relay elements are added, it may be appropriate to deal with them in a more systematic way. In this regard, some interesting investigations are reported in [16]–[19]. In more detail, in [16], the case of a multi-hop WPT link using a single transmitter and multiple receivers is discussed demonstrating that the hop count affects the power division ratio of each receiver. In [17]-[18], the case of N in-line magnetically coupled resonators is analyzed by using K-inverters to model the magnetic coupling between adjacent resonators. More specifically, in [17] it is demonstrated that at the frequency of resonance and in the case of a load and a generator having the same impedance, a lossless symmetrical WREL system with an odd number of relay resonators is always matched. Similarly, in [18], an impedance matching method is proposed in order to maximize the efficiency of the link for a generic value of N. In [19], a design approach based on the coupled resonator bandpass filter model is proposed and at the frequency of resonance of the coupled resonators the analytical expressions of the system performance are derived. Additionally, it is demonstrated that the bandwidth of a multi–hop WPT link narrows as the distance between the resonators increases.

However, studies reported in [16]–[19] focus on a single-frequency analysis. In this regard, of particular interest is the broadband investigation presented in [20] where the similarity between a multi-hop wireless link and a magneto–inductive waveguide [21] is highlighted. More specifically, in [20] a multi-hop link using N in-line identical and equally-spaced resonators is considered and analyzed on the basis of an Artificial Transmission Line (ATL) approach that exploits the properties of periodic networks [22]-[31]. The multi-hop link is modeled as a cascade of LC unit cells and in the case of identical resonators having the same mutual coupling, the existence of a pass–band characterized by negative values of the effective parameters (i.e., a Double Negative–DNG pass–band) [31] is demonstrated. In addition, it is shown that for the lossless case, a list of frequencies can be identified in the DNG pass-band where the WREL is perfectly matched independently of the impedance termination of the input and output port.

By developing the analysis presented in [20], further new significative results and considerations are presented in this paper. In particular, the analysis is extended to the case of real resonators by including loss. Useful design formulas are derived and discussed. In particular, the effective parameters

G. Monti is with the Department of Engineering for Innovation, University of Salento, Lecce, Italy, e-mail: giuseppina.monti@unisalento.it

L. Corchia is is with the Department of Engineering for Innovation, University of Salento, Lecce, Italy, e-mail: laura.corchia@unisalento.it

L. Tarricone is with the Department of Engineering for Innovation, University of Salento, Lecce, Italy, e-mail: luciano.tarricone@unisalento.it

M. Mongiardo is with the Department of Electronic and Information Engineering, University of Perugia, Perugia, Italy, e-mail: mauro.mongiardo@unipg.it

Manuscript received April, 2015; revised xx, 2016.

of the analyzed multi-hop link are calculated and a closed–form expression of the scattering parameters is derived. The proposed design formulas allow a systematic development of WPT networks possibly including several relay elements.

The paper is structured as follows: the system here considered is presented in section II and analyzed by using an ATL approach. The scattering parameters in the lossless and in the lossy case are derived in section III and IV, respectively. Comparisons with circuit simulation results and experimental data are provided in section V. Finally, conclusions are drawn in section VI.

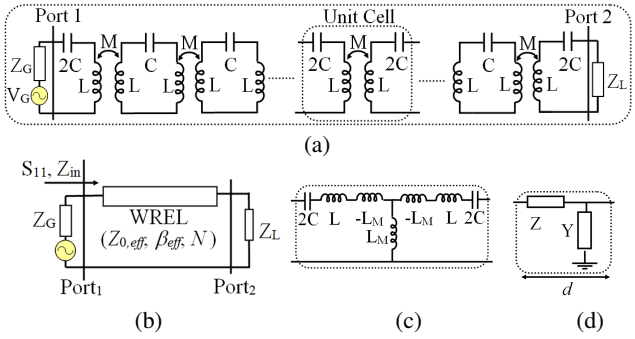

Figure 1. a) Schematic representation of the WREL system analyzed in this paper: a cascade of N inductively coupled unit cells each one consisting of an LC circuit. b) Artificial transmission line representation of the periodic network illustrated in Fig. 1a; c) equivalent circuit of the unit cell highlighted in Fig. 1a; d) unit cell representation using a generic series impedance and a generic shunt admittance.

II. Architecture of the Proposed WREL

We consider a multi-hop wireless link consisting of $(N+1)$ resonators: a transmitting (the first resonator) and a receiving resonator (the last resonator) wirelessly connected through $(N-1)$ relay elements. It is assumed that the mutual coupling between non-adjacent resonators is negligible. According to the analysis developed in [32], this hypothesis is verified in applications where the distances between every two adjacent resonators are relatively large with respect to the radius of the loops (e.g., distance/radius > 2). In fact, in these cases the mutual inductance between two non-adjacent resonators is negligible with respect to the mutual inductance between two adjacent resonators [32]. It also assumed that: 1) all the resonators are synchronous, 2) the inductive coupling between adjacent resonators is the same for all resonators, 3) the $(N-1)$ relay resonators are identical and can be modeled as an inductor of value $2L$ in series with a capacitor of value C, and 4) the transmitting and the receiving resonator are identical and can be modeled as an inductor of value L in series with a capacitor of value $2C$. According to these assumptions, the multi-hop link can be described by using the equivalent circuit illustrated in Fig. 1a. It can be noticed that the equivalent circuit is a periodic network obtained as repetition of N identical unit cells, each one associated to two adjacent resonators. In more detail, the first cell includes the first resonator (i.e., the transmitting one), half of the first relay element and the magnetic coupling between them. Similarly, the last cell includes the last resonator (i.e., the receiving one), half of the last relay element and the magnetic coupling between them. As for the generic i^{th} cell, it includes half of two consecutive relay resonators and the magnetic coupling between them. Consequently, according to hypotheses 3)-4), the N unit cells are identical. Additionally, by using inverters to model the inductive coupling between adjacent resonators, the T-network illustrated in Fig. 1c can be derived as equivalent circuit of the unit cell.

According to the detailed analysis developed in [29]-[31], in the frequency range where the phase shift associated to the unit cell is much smaller than 2π ($|\varphi_{unit\,cell}| \ll 2\pi$), the network behaves as an effectively homogeneous transmission line. In this frequency range, the network can be described by using the following effective parameters [29]-[31]:

$$\varphi_{unit\,cell} = k_{eff}d = \sqrt{-ZY}, Z_{eff} = \sqrt{\frac{Z}{Y}}\,. \tag{1}$$

In (1) k_{eff} and Z_{eff} are the effective phase propagation constant and characteristic impedance, respectively. With reference to Fig. 1d, Z and Y are the per unit cell series impedance and shunt admittance, respectively.

Furthermore, from transmission line theory, it can be demonstrated that the propagation along the network is equivalent to the propagation in a medium described by the following expression for the electric permittivity and the magnetic permeability [29]-[31]:

$$\varepsilon_{eff} = \frac{Y}{j\omega}, \mu_{eff} = \frac{Z}{j\omega}\,. \tag{2}$$

The per unit cell propagation constant $k_{eff}d$ is related to ε_{eff} and μ_{eff} by the well-known relation: $k_{eff}d = \sqrt{\varepsilon_{eff}\mu_{eff}}$. Referring to the unit cell highlighted in Fig. 1a, which consists of two inductively coupled LC resonators, the following expressions can be derived for Z and Y (see Figs. 1c–1d):

$$Z = j\omega 2\,(L - L_M) + \frac{1}{j\omega C}\,, \tag{3}$$

$$Y = \frac{1}{j\omega L_M}\,, \tag{4}$$

which leads to the following cases:

$$k_{eff}d = \pm\sqrt{2\frac{(1-M)}{M}}\sqrt{\frac{1}{f_{norm}^2} - 1} \tag{5}$$

$$Z_{eff} = \pm\omega L\sqrt{2M\,(1-M)}\sqrt{\frac{1}{f_{norm}^2} - 1} \tag{6}$$

with

$$f = 2\pi\omega,$$
$$f_0 = \frac{1}{2\pi\sqrt{2LC\,(1-M)}},$$
$$f_{norm} = \frac{f}{f_0}\,. \tag{7}$$

In (7) it has been introduced the normalized frequency (f_{norm}). L_M is the mutual inductance which depends on L

and on the coupling coefficient M:

$$L_M \quad = \quad ML,\ M \in [0,1]\,. \tag{8}$$

The absolute value of the real part of the effective propagation constant k_{eff} is illustrated in Fig. 2, and it is evident that it is equal to zero for frequencies above f_0. Furthermore, from (2) the following expressions can be derived for the effective electric permittivity and permeability:

$$\begin{aligned} \varepsilon_{eff} &= -\frac{1}{ML\left(2\pi f_0 f_{norm}\right)^2}\,, \\ \mu_{eff} &= 2L\left(1-M\right)\left(1-\frac{1}{f_{norm}^2}\right)\,. \end{aligned} \tag{9}$$

The frequency characteristics corresponding to (9) are shown in Fig. 2. For frequencies below f_0 both the effective constitutive parameters are negative, whereas for frequencies above f_0 the relative magnetic permeability becomes positive. As a consequence, the propagation along the periodic network illustrated in Fig. 1 is allowed only for frequencies lower than f_0 and is characterized by negative values of the real part of the effective phase propagation constant and positive values of the effective characteristic impedance (i.e., in (5) and (6) the negative and the positive sign of the square root must be taken, respectively) [31] :

$$\begin{aligned} k_{eff}d &= -\left|\sqrt{2\frac{(1-M)}{M}}\sqrt{\frac{1}{f_{norm}^2}-1}\right| = \beta_{eff}d, \\ Z_{eff} &= +\omega L\sqrt{2M\left(1-M\right)}\sqrt{\frac{1}{f_{norm}^2}-1} = Z_{eff}. \end{aligned} \tag{10}$$

In fact, the WREL illustrated in Fig. 1 behaves as a DNG medium below f_0, whereas it behaves as an epsilon negative medium above f_0.

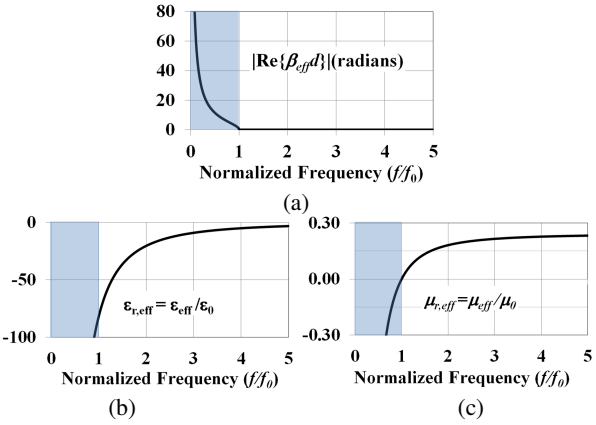

Figure 2. Effective parameters of the periodic network illustrated in Fig. 1: a) real part of the phase propagation constant; b) relative electric permittivity; c) relative magnetic permeability.

III. Scattering Parameter Determination: Lossless case

In order to use the network of Fig. 1 for WPT applications, we need to determine its transmission coefficient; to this end, we consider the WREL configured as illustrated in Fig. 1b. We assume that it consists of the cascade of N unit cells, and according to the analysis developed in the previous section it is modeled as an ATL described by effective parameters. For a lossless system the following expressions can be derived for the scattering parameters of the network when the same reference impedance is assumed at port 1 and at port 2 ($Z_L = Z_G = Z_0$):

$$|S_{21}|^2 = 1-|S_{11}|^2,\ S_{11} = S_{22} = \frac{Z_{in}-Z_0}{Z_{in}+Z_0} \tag{11}$$

where, Z_{in} is the input impedance of the WREL when it is terminated on a load impedance $Z_L = Z_0$:

$$\begin{aligned} Z_{in} &= Z_{eff}\frac{Z_0 + j\tan\left(k_{eff}dN\right)Z_{eff}}{Z_{eff}+j\tan\left(k_{eff}dN\right)Z_0} = \\ &= Z_{0|k_{eff}dN=m\pi} \end{aligned} \tag{12}$$

consequently, for the scattering parameters, we get:

$$S_{11} = S_{22} = 0\ when\ k_{eff}dN = m\pi,\ m \in \Im. \tag{13}$$

In the above expressions N is the number of unit cells (see Fig. 1). Equation (11) highlights that solving the WREL of Fig. 1 as an ATL described by effective parameters leads to the well know behaviour of a conventional transmission line: for any value of Z_0 and Z_{eff} the WREL is perfectly matched at all frequencies corresponding to a phase shift multiple of π. By using (5)–(7), it can be derived that these frequencies are given by:

$$\tilde{f}_{norm,m} = \frac{1}{\sqrt{\frac{M}{2(1-M)}\left(\frac{m\pi}{N}\right)^2+1}},\ m \in \Im. \tag{14}$$

It is worth observing that for any m, N and M, these frequencies are lower than the upper bound f_0 of the WREL pass-band. On the other hand, it should be considered that for frequencies lower than f_0 the phase-shift of the unit cell is smaller than π and then the phase shift of the cascade of N unit cells is smaller than $N\pi$. Additionally, from Fig. 2a it can be seen that the phase shift of the ATL increases as the frequency decreases, therefore the upper bound on the phase shift leads to the following lower bound for the frequencies $\widetilde{f}_{norm,m}$:

$$f_{low} = \frac{1}{\sqrt{\frac{M}{2(1-M)}\pi^2+1}}. \tag{15}$$

Consequently, the network of Fig. 1 consisting of N identical unit cells exhibits a list of $(N-1)$ frequencies where it is perfectly matched with respect to a generic reference impedance, i.e.:

$$S_{11} = S_{22} = 0$$

when

$$f_{norm} = \widetilde{f}_{norm,m} \in \left(f_{low}, 1\right),\ m \in \left[1,\ (N-1)\right]. \tag{16}$$

Considering that the network of Fig. 1 represents a WREL system consisting of a transmitting and a receiving resonator connected through $(N-1)$ relay elements, it can be concluded that the number of matching frequencies is equal to the number of relay resonators.

IV. Lossy Case

The results obtained in the previous section can be easily extended to the case of a WREL consisting of magnetically coupled lossy LC resonators by adding to the equivalent circuit of Fig. 1 a series resistance R. In more detail, we add a resistance of value $R/2$ in series configuration to the LC resonators of the two branches of the T-network illustrated in Fig. 1c. As a consequence, in the lossy case (3)–(5) modify as follows:

$$\begin{aligned} Z &= R + j\omega 2\left(L - L_M\right) + \frac{1}{j\omega C}, \\ Y &= \frac{1}{j\omega L_M}, \\ k_{eff,L} &= \beta_{eff,L} - j\alpha_{eff} = \\ &= \pm\sqrt{2\frac{(1-M)}{M}\left(\frac{1}{f_{norm}^2} - 1\right)} \times (\sqrt{1+j\xi})_{1/2}, \\ \xi &= \frac{f_{norm}}{Q\left(1 - f_{norm}^2\right)}, \\ Q &= \frac{4\pi f_0 L\left(1-M\right)}{R}. \end{aligned} \tag{17,18}$$

Where, the subscript L is used to indicate that we are dealing with the lossy case, while the subscript $1/2$ indicates the two possible solutions of the complex square root $\sqrt{1+j\xi}$. Additionaly, in (18) the dependence of the propagation constant on the quality factor Q of the series resonator of the unit cell (see Fig. 1c) is highlighted. In order to fully specify $k_{eff,L}$, a physical choice has to be made for the solution of the two square roots appearing in (18). In this regard, it should be considered that for $R \to 0$ we must recover the expression of k_{eff} calculated for the lossless case and given in (10). Accordingly, the solution with a negative sign has to be taken for the first square root. As for the square root $\sqrt{1+j\xi}$, it admits the following solutions:

$$\sqrt{1+j\xi} = \begin{bmatrix} \nu_1 \\ \nu_2 \end{bmatrix} = \\ = \begin{bmatrix} \sqrt{1+\xi^2} \times \left[cos\left(\frac{\xi}{2}\right) + jsin\left(\frac{\xi}{2}\right)\right] \\ \\ \sqrt{1+\xi^2} \times \left[cos\left(\frac{\xi}{2}+\pi\right) + jsin\left(\frac{\xi}{2}+\pi\right)\right] \end{bmatrix}. \tag{19}$$

In this case, the solution to be taken is the one which guarantees a result consistent with the propagation in a passive medium characterized by positive values of the attenuation constant α_{eff}. According to this consideration, and taking into account that the negative sign has been selected for the first square root, it can be derived that the solution corresponding to a positive imaginary part has to be taken for $\sqrt{1+j\xi}$. From (19), it can be seen that the solution corresponding to a positive imaginary part is ν_1 for $\xi > 0$, while it is ν_2 for $\xi < 0$. Additionally, from (18) it can be noticed that ξ is always positive in the frequency range where the propagation along the WREL is allowed (i.e., $f_{norm} < 1$); therefore, to obtain for $k_{eff,L}$ a result consistent with the propagation in a passive medium, the solution ν_1 has to be selected in (19):

$$\sqrt{1+j\xi} = \nu_1 = \sqrt{1+\xi^2} \times \left[cos\left(\frac{\xi}{2}\right) + jsin\left(\frac{\xi}{2}\right)\right]. \tag{20}$$

According to the above reported considerations, for the effective propagation constant and characteristic impedance we get:

$$k_{eff,L}d = \beta_{eff}d \times \nu_1 \tag{21}$$

$$Z_{eff,L} = Z_{eff} \times \nu_1 \tag{22}$$

where $\beta_{eff}d$ and Z_{eff} are the effective phase propagation constant and characteristic impedance calculated in the lossless case (10).

In most cases of practical interest, the LC resonators satisfy the small loss condition:

$$|\xi| \ll 1 \tag{23}$$

and simple closed forms of the effective parameters of the ATL can be derived by approximating the square root $\sqrt{1+j\xi}$ by its Taylor polynomial of degree n centered at $\xi = 0$:

$$\sqrt{1+j\xi} \approx \\ = 1 + j\tfrac{\xi}{2} + ... + \frac{\prod(\frac{1}{2}-l+1)_{l=1,n}}{n!}\xi^n + o\left(\xi^n\right). \tag{24}$$

Results obtained in the case of a second– and first– order approximation are presented and discussed in the following part of this section.

A. Small loss: Second Order Approximation

Let us approximate the square root $\sqrt{1+j\xi}$ by its Taylor polynomial of degree 2:

$$\sqrt{1+j\xi} \approx 1 + j\frac{\xi}{2} + \frac{\xi^2}{8} + o\left(\xi^3\right) = T_2 \tag{25}$$

and then for the propagation constant we get:

$$\begin{aligned} k_{eff,L}d &= \beta_{eff,L}d - j\alpha_{eff}d = \\ &\approx \left|\left[\sqrt{2\frac{(1-M)}{M}}\sqrt{\frac{1}{f_{norm}^2} - 1}\right]\right| \times T_2 \\ \beta_{eff,L}d &\approx \beta_{eff}d \times \left(1 + \frac{\xi^2}{8}\right) + o(\xi^4), \\ \alpha_{eff}d &\approx \beta_{eff}d \times \frac{\xi}{2} + o(\xi^3). \end{aligned} \tag{26}$$

With respect to the lossless case, from (26) it can be noticed that the presence of loss affects both the real and the imaginary part of the propagation constant. In particular, this leads to an imaginary part different from zero, and thus corresponding to an attenuation experienced by the propagating signal. Furthermore, from (26) it can be seen that the use of a second order approximation for $\sqrt{1+j\xi}$ introduces an error on both the real and imaginary part of $k_{eff,L}d$. This error is proportional to ξ^4 for $\beta_{eff,L}d$, while it is proportional to ξ^3 for $\alpha_{eff}d$.

Similarly, the effective characteristic impedance becomes:

$$\begin{aligned} Z_{eff,L} &= R_{0,eff} + jX_{0,eff} = Z_{eff} \times T_2, \\ R_{0,eff} &= Z_{eff} \times \left(1 + \frac{\xi^2}{8}\right) + o(\xi^4), \\ X_{0,eff} &= Z_{eff} \times \frac{\xi}{2} + o(\xi^3). \end{aligned} \quad (27)$$

B. Small loss: First Order Approximation

Let us now approximate the square root $\sqrt{1+j\xi}$ by its Taylor polynomial of degree 1:

$$\sqrt{1+j\xi} \approx 1 + j\frac{\xi}{2} + o\left(\xi^2\right) = T_1 \quad (28)$$

By using (28) in (18) for the propagation constant we get:

$$\begin{aligned} k_{eff,L}d &= \beta_{eff,L}d - j\alpha_{eff}d = \\ &\approx \left|\left[\sqrt{2\frac{(1-M)}{M}}\sqrt{\frac{1}{f_{norm}^2} - 1}\right]\right| \times T_1 \\ \beta_{eff,L}d &\approx \beta_{eff}d + o(\xi^2), \\ \alpha_{eff}d &\approx \beta_{eff}d \times \frac{\xi}{2} + o(\xi^3). \end{aligned} \quad (29)$$

From (29), it can be seen that by using a first order approximation of the square root $\sqrt{1+j\xi}$ the error on $\beta_{eff,L}d$ is proportional to ξ^2 while the error on $\alpha_{eff}d$ is proportional to ξ^3. It can be also noticed that, in this case, the real part of the propagation constant is the same calculated for the lossless case: the presence of loss only leads to the presence of an imaginary part that is the same calculated by using a second–order approximation.

As for the effective characteristic impedance, we obtain:

$$\begin{aligned} Z_{eff,L} &= R_{0,eff} + jX_{0,eff} = Z_{eff} \times T_1, \\ R_{0,eff} &= Z_{eff} + o(\xi^2), \\ X_{0,eff} &= Z_{eff} \times \frac{\xi}{2} + o(\xi^3). \end{aligned} \quad (30)$$

C. Scattering Parameters determination

According to results reported in the previous part of this section, the input impedance of the lossy WREL becomes:

$$\begin{aligned} Z_{in,L} &= Z_{eff,L}\frac{Z_0 + \tanh\left(k_{eff,L}dN\right) Z_{eff,L}}{Z_{eff,L} + \tanh\left(k_{eff,L}dN\right) Z_0} \\ &= Z_{eff,L}\frac{1 + \Gamma_0 e^{-2\alpha_{eff}dN} e^{-j2\beta_{eff,L}dN}}{1 - \Gamma_0 e^{-2\alpha_{eff}dN} e^{-j2\beta_{eff,L}dN}}, \\ \Gamma_0 &= \frac{Z_{eff,L} - Z_0}{Z_{eff,L} + Z_0}. \end{aligned} \quad (31)$$

where $k_{eff,L}$ and $Z_{eff,L}$ can be expressed by using the exact solution given in (21)-(22). Alternatively, if the small loss condition is satisfied, the second– or first–order approximated expressions given in (26)-(27) and in (29)-(30) can be used.

As for the scattering parameters, the reflection coefficients S_{11} and S_{22} can be calculated by using (11) with $Z_{in,L}$ in place of Z_{in}. As can be derived from (31), in the lossy case (12) is no longer valid; as a consequence, at the frequencies $\tilde{f}_{norm,m}$ the analyzed WREL is not perfectly matched with respect to a generic impedance, and the presence of reflections must be taken into account. However, the magnitude of these reflections is increasingly negligible as is true the hypothesis of small loss. In fact, from (31) it can be seen that under the small loss condition and for $f = \tilde{f}_{norm,m}$ the input impedance $Z_{in,L}$ assumes values very close to the reference impedance Z_0. In this case, the frequencies $\tilde{f}_{norm,m}$ are the frequencies of the relative minima of the S_{11} parameter.

Finally, both the presence of reflections and of an attenuation factor must be taken into account in calculating the transmission coefficient S_{21}:

$$|S_{21}| = \sqrt{1 - \left|\frac{Z_{in,L} - Z_0}{Z_{in,L} + Z_0}\right|^2} \times exp(-\alpha_{eff}dN)\,. \quad (32)$$

In the following, analytical formulas discussed in this section will be validated by comparisons with circuital simulations and experimental data.

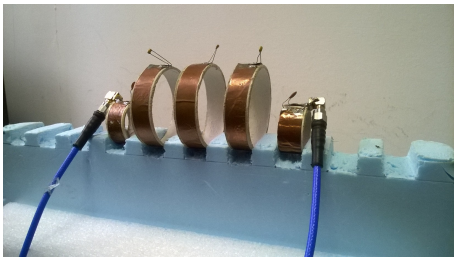

Figure 3. Photograph of the WREL system analyzed in section V. It consists of five capacitively loaded loops coupled by their electromagnetic field. The first and last resonators have a diameter of 2.6 cm and a loading capacitor of 82 pF, while the relay resonators have a diameter of 5.4 cm and a loading capacitor of 39 pF. The distance between each resonator and the preceding one is 1.5 cm

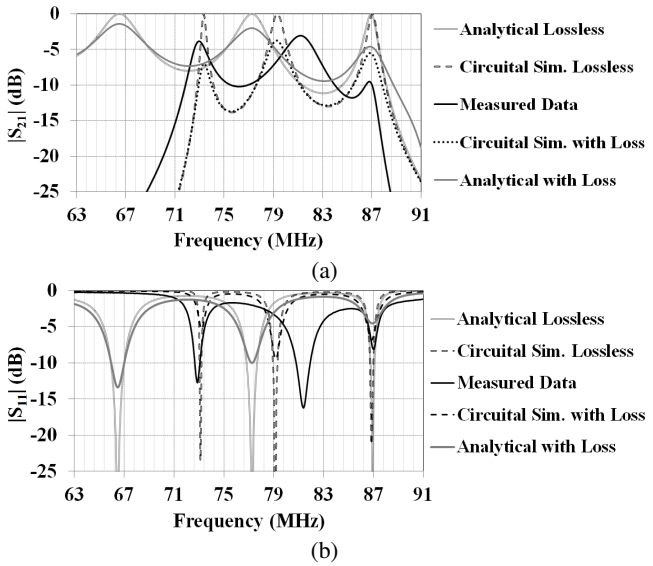

Figure 4. Comparison between analytical, simulated and experimental data of the WREL of Fig. 3. Results obtained for the S_{21} (a) and the S_{11} parameter (b). Although there is not a precise agreement between measured and analytical data, it can be observed that the frequency behaviour of the S_{21} and S_{11} parameters is qualitatively the same. Measured data confirm that the WREL system exhibits a number of matching frequencies that is equal to the number of relay resonators.

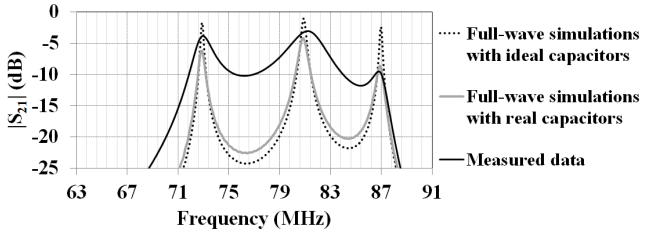

Figure 5. Comparison between numerical and experimental data of the WREL of Fig. 3. Full–wave simulations were performed both for the case of ideal capacitors and the case of real capacitors with a finite Q factor (simulations were performed by using an equivalent series resistance of $0.1\,\Omega$ for the relay resonators and of $0.05\,\Omega$ for the first and last resonators).

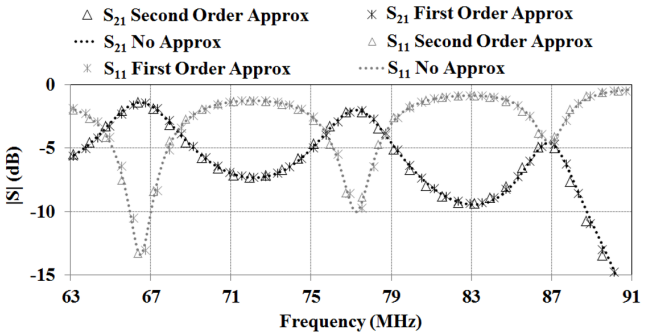

Figure 6. Comparison between analytical data obtained for the WREL illustrated in Fig. 3 by using different order of approximation for the square root $\sqrt{1+j\xi}$.

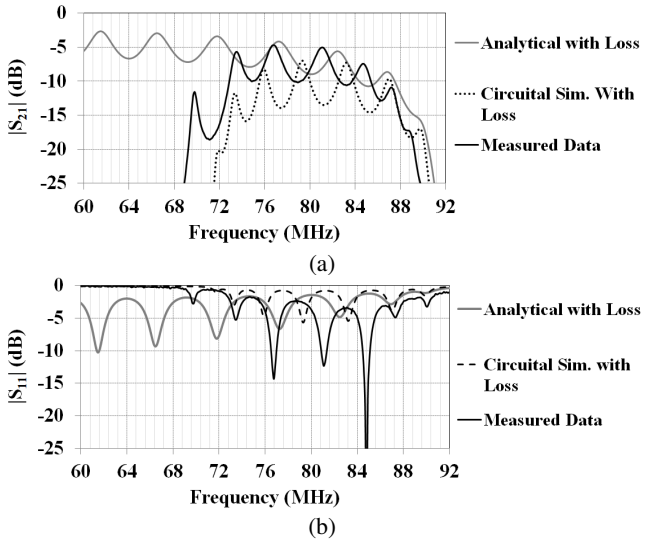

Figure 7. Analytical, simulated and experimental data obtained by adding four relay resonators to the WREL of Fig. 3. (a) Results obtained for the S_{21} parameter, (b) results obtained for the S_{11} parameter. Analytical data and circuital simulations were calculated for the lossy case by using a value of $0.4\,\Omega$ for R.

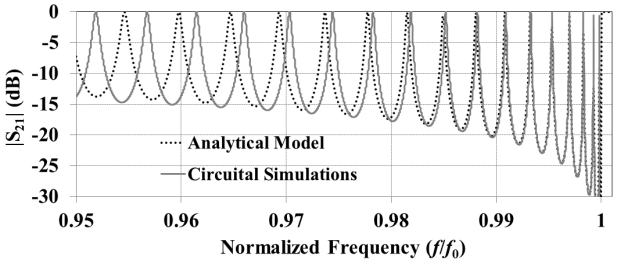

Figure 8. S_{21} parameter of a lossless WREL consisting of 64 unit cells (i.e., 65 resonators): comparison between circuital simulations and results obtained by using (11). The unit cell parameters are: $L = 49\,\mathrm{nH}$, $L_M = 11.8\,\mathrm{nH}$, $C = 39\,\mathrm{pF}$.

V. Results

In order to verify the suitability of using the proposed ATL approach for the analysis of a multi–hop inductive wireless power link, results obtained by means of analytical formulas were compared with circuital simulations and experimental data. Experiments were performed for the WREL illustrated in Fig. 3 which consisted of five resonators: a transmitter and a receiver connected through 3 relay elements. Each resonator was a loop loaded with a lumped capacitor and was fabricated using a cardboard tube as support and adhesive copper strips. The parameters of the copper strips were: width = $12\,\mathrm{mm}$, thickness = 0.035 mm, conductivity = 5.8×10^8 S/m. In order to accurately reproduce the periodic network illustrated in Fig. 1 and analyzed in the previous sections, the first and last resonators were fabricated so to have an inductance half of that corresponding to the central resonators (i.e., the relay resonators). Similarly, the capacitor used as loading capacitor for the first and last resonators approximately doubled that used for the relay resonators. In more detail, the first and last resonators had a diameter of $2.6\,\mathrm{cm}$ and a loading capacitor of $82\,\mathrm{pF}$, while the relay resonators had a diameter of $5.4\,\mathrm{cm}$ and a loading capacitor of $39\,\mathrm{pF}$; the distance between each resonator and the preceding one was $1.5\,\mathrm{cm}$. Referring to Fig. 1, the system illustrated in Fig. 3 is equivalent to an ATL consisting of 4 unit cells (i.e., the number of resonators minus one). The R & S ZVL6 VNA (Vector Network Analyzer) was used for scattering parameters measurements; semi-rigid coaxial cables (UT141) with $50\,\Omega$ SMA connectors were employed for connecting the WREL to the VNA. A short, open, load and through calibration technique was adopted for all measurements presented in this work.

With reference to the equivalent circuit illustrated in Fig. 1, a first set of measurements was performed in order to determine the unit cell parameters. More specifically, the equivalent inductance of each resonator was determined through measurements of the reflection coefficient. As for the mutual coupling between adjacent resonators, it was determined by fitting circuital simulation results and measurements. In more detail, circuital simulations were performed in order to calculate the transmission coefficient of the equivalent circuit illustrated in Fig. 1 for different values of the number of unit cells N. Similarly, measurements were performed by varying the number of relay elements interposed between the transmitting and the receiving resonators while keeping at $1.5\,\mathrm{cm}$ the

mutual distance between adjacent resonators. The value of the mutual coupling M was set to guarantee the best fitting between simulated and measured data. This way, the following values were obtained for the unit cell parameters: $L \approx 49\,\mathrm{nH}$, $L_M \approx 11.8\,\mathrm{nH}$, $M \approx 0.24$, thus corresponding to a value for f_0 of about $91.08\,\mathrm{MHz}$. These data were used for calculating the scattering parameters of the WREL illustrated in Fig. 1 according to the ATL theoretical model presented in the previous sections. In Fig. 4, the obtained results are compared with circuital simulations and measurements. Analytical and circuital simulations data are reported for both the lossless and lossy case. A value of $0.4\,\Omega$ was assumed for R for the lossy case, thus corresponding to a value of the resonators Q factor of about 107. In order to investigate the physical phenomena determining the value of R (i.e., the system loss), full–wave simulations were performed by using the commercial software CST Microwave studio. From full–wave simulations it was derived that the system loss is mainly due to three different contributions: the materials adopted for fabrication (i.e., the finite conductivity of the copper tape and the non zero conductivity of the cardboard tube), proximity effects resulting in a non-uniform current density across the cross section of the resonators, and the Q factor of the lumped capacitors. In more detail, a first set of simulations was performed by neglecting the loss of the lumped capacitors. Starting from these results, the Q factor of the lumped capacitors was determined by fitting numerical and measured data. The transmission coefficient obtained this way for the WREL illustrated in Fig. 3 is reported in Fig. 5. The results obtained for both the case of ideal lumped capacitors and the case of capacitors having a Q factor of about 448 are reported. These results highlight the loss due to the materials adopted for fabrication and to proximity effects (see the curve referring to ideal capacitors). This loss could be reduced by using Litz wires to build the coils [5], [33].

With regard to loss, analytical data reported for the lossy case in Fig. 4 were calculated by using the exact solution of the square root $\sqrt{1+j\xi}$. According to the discussion developed in the previous section, a comparison of analytical data corresponding to different approximations of $\sqrt{1+j\xi}$ is given in Fig. 6. It can be seen that results obtained by using a second– and a first–order approximation are in very good agreement with those obtained by using the exact solution of the square root $\sqrt{1+j\xi}$. This demonstrates that, for the considered case, a first–order approximation provides a good accuracy in calculating the scattering parameters.

Experiments were also performed by adding four relay resonators to the WREL illustrated in Fig. 3, and thus corresponding to an ATL consisting of 8 unit cells. In Fig. 7, the measured scattering parameters are compared with analytical and simulated results.

Observing Fig. 4, it can be seen that from simulated and experimental data the WREL using 5 resonators, and thus corresponding to an ATL consisting of 4 unit cells, exhibits 3 minima of the reflection coefficient and that these minima are below $f = 91.08$ MHz corresponding to $f_{norm} = 1$. Similarly, observing Fig. 7, it can be seen that from simulated and experimental data, the WREL using 9 resonators, and thus corresponding to an ATL consisting of 8 unit cells, exhibits 7 minima of the reflection coefficient and that also in this case these minima are below $f_{norm} = 1$. These results confirm that a WREL using $(N+1)$ resonators exhibits $(N-1)$ matching frequencies, thus validating the analytical result summarized in (16). From Fig. 4 and Fig. 7, it can be also noticed that analytical data are in fairly good agreement with simulated and measured data in the upper part of the bandwidth. The agreement worsens as the frequency decreases. This result is a direct consequence of an intrinsic limit of the ATL model, which assumes that the unit cell phase shift is much smaller than 2π. This hypothesis limits the validity of the model to frequencies corresponding to a phase-shift of the unit cell at least lower than $\pi/4$. As a consequence, (14) provides a good accuracy in calculating the frequencies $\widetilde{f}_{norm,m}$ for $m < N/4$. These considerations were verified by means of circuital simulations: Fig. 8 compares results obtained by means of circuital simulations and the ones corresponding to the ATL analytical model in the case of a WREL consisting of 65 resonators (i.e., equivalent to an ATL of 64 unit cells). The unit cell parameters are the same corresponding to the WREL of Fig. 3 (i.e., $L = 49\,\mathrm{nH}$, $L_M = 11.8\,\mathrm{nH}$, $C = 39\,\mathrm{pF}$). It can be seen that a good agreement was obtained for $\widetilde{f}_{norm,m} < 0.95$ which is the normalized frequency corresponding to $\widetilde{f}_{norm,m=N/4=16} = 0.954$. According to these considerations, it can be concluded that a viable solution for extending the frequency range where the analytical model provides a good accuracy is represented by the use of a unit cell with a a phase delay as small as possible in the frequency range of interest.

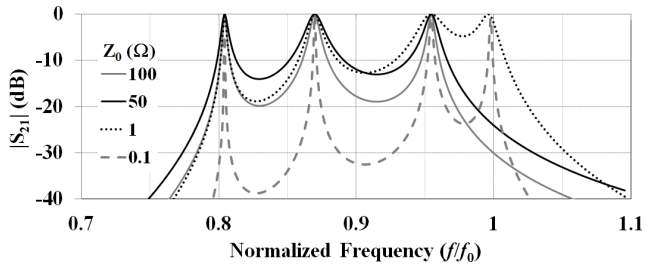

Figure 9. Circuital simulation results obtained for different values of the reference impedance Z_0.

Further investigations for the WREL of Fig. 1 were performed by means of both circuital simulations and experiments; the corresponding results are given in Figs. 9-10. In particular, Fig. 9 shows the results obtained for the WREL of Fig. 3 for different values of the port reference impedance ($Z_L = Z_G = Z_0$). In agreement with (16), for all the analyzed values of Z_0 and below f_0, the WREL exhibits a perfect matching at a number of $(N-1) = 3$ frequencies. Furthermore, it can be noticed that for small values of Z_0, the WREL is matched also to a fourth frequency, which approaches to f_0 as Z_0 approaches to zero. This result is in agreement with (7), (11); in fact, it can be noticed that the WREL effective characteristic impedance, and then its input impedance, approaches to zero when the frequency approaches to f_0:

$$Z_{eff} \underset{f \to f_0}{\to} 0 \Rightarrow Z_{in} \underset{f \to f_0}{\to} 0$$

The effect of the coupling factor M on the WREL pass–band is highlighted in Fig. 10. In more detail, Fig. 10a shows circuital simulation results calculated by varying the coupling factor M of a WREL consisting of four unit cells with $L = 49\,\mathrm{nH}$, $C = 39\,\mathrm{pF}$, $R = 0.4\,\Omega$. Figure 10b illustrates experimental data obtained for the WREL illustrated in Fig. 3. In this case, in order to investigate the effect of the coupling factor on the transmission coefficient, measurements were performed for different values of the distance between two consecutive resonators. From Fig. 10, it can be seen that circuital and experimental data are in good agreement. In fact, in both cases it can be seen that higher values of M correspond to a wider bandwidth. This is in agreement with the upper and lower bound determined in section III for the $\widetilde{f}_{norm,m}$. In fact, from (15) it can be derived that the lower bound (f_{low}) approaches to the upper bound (f_0) as M approaches to zero. Conversely, when M approaches to 1, f_{low} approaches to zero and f_0 approaches to ∞.

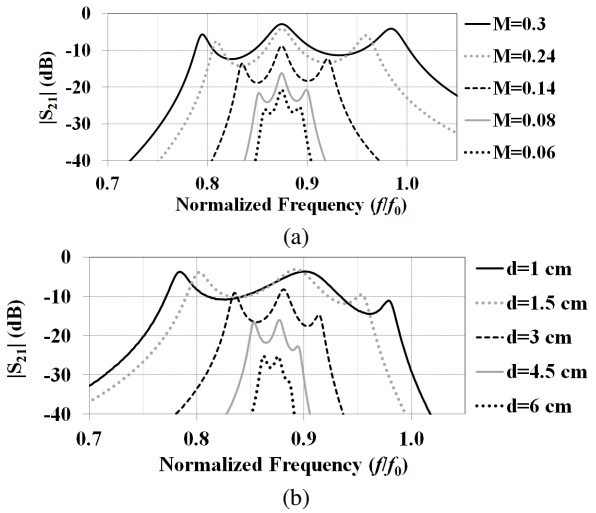

Figure 10. Results obtained for different values of the coupling factor M. (a) Circuital simulation results obtained for a WREL consisting of four unit cells with: $L = 49\,\mathrm{nH}$, $C = 39\,\mathrm{pF}$, $R = 0.04\,\Omega$. (b) Experimental data obtained by varying the distance (d) among the resonators of the WREL illustrated in Fig. 3.

VI. Conclusion

A multi–hop wireless system consisting of a cascade of inductively coupled resonators was investigated. The general case of a link consisting of $(N + 1)$ resonators, a transmitting and a receiving resonator connected through $(N - 1)$ relay elements, was considered. By using an artificial transmission line approach, useful design formulas that allow linking the frequency behaviour of the WPT system to its parameters were derived and discussed.

In particular, it was demonstrated that the analyzed multi–hop wireless link exhibits a pass–band characterized by negative values of the effective parameters. The frequency behaviour corresponding to analytical formulas was validated by comparisons with experimental data and circuital simulation results.

Reported results highlight the convenience of using relay resonators in wireless energy links. In fact, as demonstrated in this paper, a multi–hop wireless link using $(N - 1)$ relay elements exhibits $(N - 1)$ frequency values, for which it is perfectly matched with respect to a generic termination.

It can therefore be concluded that the use of relay elements, beside extending the distance covered by the wireless link, extends its operating bandwidth by adding frequencies useful for power transmission.

References

[1] A. Kurs, A. Karalis, R. Moffatt, J. D. Joannopoulos, P. Fisher, and M. Soljacic, "Wireless power transfer via strongly coupled magnetic resonances," *Science*, vol. 317, no. 5834, pp. 83–86, July 2007.

[2] A. Costanzo, M. Dionigi, M. Masotti, M. Mongiardo, G. Monti, L. Tarricone, and R. Sorrentino, "Electromagnetic energy harvesting and wireless power transmission: A unified approach," *Proceedings of the IEEE*, vol. 102, no. 11, pp. 1692–1711, November 2014.

[3] G. Monti, L. Corchia, and L. Tarricone, "A wearable wireless energy link," in *45th European Microwave Conference*, 2015, pp. 143–146.

[4] C. Zhu, C. Yu, K. Liu, and R. Ma, "Research on the topology of wireless energy transfer device," in *Vehicle Power and Propulsion Conference (VPPC '08). IEEE*, Harbin, Heilongjiang, China, October 2008.

[5] Z. N. Low, R. A. Chinga, R. Tseng, and J. Lin, "Design and Test of a High-Power High-Efficiency Loosely Coupled Planar Wireless Power Transfer System," *IEEE Trans. on Industrial Electronics*, vol. 56, no. 5, pp. 1801–1812, May 2009.

[6] C.-J. Chen, T.-H. Chu, C.-L. Lin, and Z.-C. Jou, "A Study of Loosely Coupled Coils for Wireless Power Transfer," *IEEE Trans. on Circuits and Systems II: Express Briefs*, vol. 57, no. 7, pp. 536–540, July 2010.

[7] B. L. Cannon, J. F. Hoburg, D. D. Stancil, and S. C. Goldstein, "Magnetic Resonant Coupling As a Potential Means for Wireless Power Transfer to Multiple Small Receivers," *IEEE Trans. on Power Electronics*, vol. 24, no. 7, pp. 1819–1825, July 2009.

[8] A. Costanzo, M. Dionigi, F. Mastri, and M. Mongiardo, "Wireless resonant-type power transfer links with relay elements: Harmonic balance design," in *42nd European Microwave Conference*, Amsterdarm, Netherlands, October 2012, pp. 225–228.

[9] A. P. Sample, D. A. Meyer, and J. R. Smith, "Analysis, Experimental Results, and Range Adaptation of Magnetically Coupled Resonators for Wireless Power Transfer," *IEEE Trans. on Industrial Electronics*, vol. 58, no. 2, pp. 544 – 554, February 2011.

[10] G. Monti, , L. Tarricone, and C. Trane, "Experimental characterization of a 434 MHz wireless energy link for medical applications," *Progress In Electromagnetics Research C*, vol. 30, pp. 53–64, 2012.

[11] G. Monti, P. Arcuti, and L. Tarricone, "Resonant Inductive Link for Remote Powering of Pacemakers," *IEEE Trans. on Microwave Theory and Techniques*, vol. 63, no. 11, pp. 3814–3822, November 2015.

[12] M. Dionigi and M. Mongiardo, "Cad of wireless resonant energy links (wrel) realized by coils," in *IEEE MTT-S International Microwave Symposium Digest*, Anaheim, CA, May 2010, pp. 1760–1763.

[13] T. Sun, X. Xie, G. Li, Y. Gu, Y. Deng, and Z. Wang, "System with an efficiency-enhanced power receiver for motion-free capsule endoscopy inspection," *IEEE Trans. on Biomedical Engineering*, vol. 59, no. 11, pp. 3247–3253, November 2012.

[14] W. Zhong, C. Zhang, X. Liu, and S. Hui, "A methodology for making a three-coil wireless power transfer system more energy efficient than a two-coil counterpart for extended transfer distance," *IEEE Trans. on Power Electronics*, vol. 30, no. 2, pp. 3288 – 3297, February 2015.

[15] D. Ahn and S. Hong, "A study on magnetic field repeater in wireless power transfer," *IEEE Trans. on Industrial Electronics*, vol. 60, no. 1, pp. 360 – 371, January 2013.

[16] A. Shimada, Y. Ito, H. Uehara, and T. Ohira, "Effect of hop counts on power division ratio in multi-hop power transfer via magnetic resonance," in *IEEE Wireless Power Transfer Conference 2013*, Perugia, Italy, 2013, pp. 179–184.

[17] M. Dionigi and M. Mongiardo, "Magnetically coupled resonant wireless power transmission systems with relay elements," in *Microw. Workshop Series on Innovative Wireless Power Transmission: Technologies, Systems, and Applications*, Kyoto, May 2012.

[18] Y. Narusue, Y. Kawahara, and T. Asami, "Impedance Matching Method for Any-Hop Straight Wireless Power Transmission Using Magnetic Resonance," in *IEEE Radio Wireless Week*, Phoenix, Arizona, 2013, pp. 193–195.

[19] B. Luo, S. Wu, and N. Zhou, "Flexible design method for multi-repeater wireless power transfer system based on coupled resonator bandpass filter model," *IEEE Trans. on Circuits and Systems-I: Regular Papers*, vol. 61, no. 11, pp. 933 – 942, November 2014.

[20] G. Monti, L. Tarricone, M. Dionigi, and M. Mongiardo, "Magnetically coupled resonant wireless power transmission: An artificial transmission line approach," in *42nd Microwave Conference*, Amsterdarm, Netherlands, October 2012, pp. 233–236.

[21] E. Shamonina, V. A. Kalinin, K. H. Ringhofer, and L. Solymar, "Magneto-inductive waveguide," *Electron. Lett.*, vol. 38, pp. 371–373, 2002.

[22] G. Monti and L. Tarricone, "Signal reshaping in a transmission line with negative group velocity behaviour," *Microwave and Optical Technology Letters*, vol. 51, no. 11, pp. 2627–2633, November 2009.

[23] ——, "Dual-band artificial transmission lines branch-line coupler," *Int. Journal of RF and Microwave Computer-Aided Engineering*, vol. 18, no. 1, pp. 53–62, September 2007.

[24] A. Sanada, C. Caloz, and T. Itoh, "Characteristics of the composite right/left-handed transmission lines," *IEEE Microwave and Wireless Components Lett.*, vol. 14, no. 2, pp. 68–70, March 2004.

[25] J. J. Sanchez-Martinez, E. Marquez-Segura, P. Otero, and C. Camacho-Penalosa, "Artificial transmission line with left/right-handed behavior based on wire bonded interdigital capacitors," *Progress In Electromagnetics Research B*, vol. 11, pp. 245–264, 2009.

[26] I.-H. Lin, M. DeVincentis, C. Caloz, and T. Itoh, "Arbitrary dual-band components using composite right/left-handed transmission lines," *IEEE Trans. on Microwave Theory and Techniques*, vol. 52, no. 4, pp. 1142–1149, April 2007.

[27] G. Monti and L. Tarricone, "Compact broadband monolithic 3-db coupler by using artificial transmission lines," *Microwave and Optical Technology Lett.*, vol. 50, no. 10, pp. 2662–2667, October 2008.

[28] K. W. Eccleston, L. Fan, and S. H. M. Ong, "Compact planar microstripline branch-line and rat-race couplers," *IEEE Trans. On Microw. Theory and Techn.*, vol. 51, no. 10, pp. 2119–2125, October 2003.

[29] C. Caloz and T. Itoh, "Transmission line approach of left-handed (lh) materials and microstrip implementation of an artificial lh transmission line," *IEEE Trans. on Antennas and Propagation*, vol. 52, no. 5, pp. 1159–1166, May 2004.

[30] G. Monti and L. Tarricone, "Reduced-size broadband crlh-atl rat-race coupler," in *36th European Microwave Conference*, Manchester, United Kingdom, 2006, pp. 125–128.

[31] C. Caloz and T. Itoh, *Electromagnetic Metamaterials: Transmission Line Theory and Microwave Applications*. Wiley, 2005.

[32] C. K. Lee, W. X. Zhong, and S. Y. R. Hui, "Effects of Magnetic Coupling of Nonadjacent Resonators on Wireless Power Domino-Resonator Systems," *IEEE Trans. on Power Electronics*, vol. 27, no. 4, pp. 1905–1916, April 2012.

[33] J. Casanova, Z. Low, and J. Lin, "Design and Optimization of a Class-E Amplifier for a Loosely Coupled Planar Wireless Power System," *IEEE Trans. on Circuits and Systems II*, vol. 56, no. 11, pp. 830–834, November 2009.

Giuseppina Monti received the Laurea degree in Telecommunication Engineering (with honors) from the University of Bologna, Italy, in 2003, and the Ph.D. in Information Engineering from University of Salento (Italy), in 2007. She is currently with the Department of Innovation Engineering (University of Salento), where she is a temporary researcher and lecturer in CAD of Microwave circuits and Antennas. Her current research interest includes the analysis and applications of artificial media (such as, for instance, double-negative metamaterials and nano-carbontube), the analysis of electromagnetic compatibility and electromagnetic interference problems in planar microwave circuits, the design and realization of: microwave components and MEMS-based reconfigurable antennas and devices, rectenna systems, systems and devices for wireless power transmission applications. She has co-authored a chapter of a book and about 100 papers appeared in international conferences and journals.

Laura Corchia was born in Italy, in 1980. She received the M.S. degree in Telecommunication Engineering and the Ph.D in Information Engineering from University of Salento, Lecce, Italy, in 2007 and 2011, respectively. She is currently a Research Fellow with the Department of Engineering for Innovation, University of Salento. Her research interests include the development of near and far field wireless power transfer links and power management units for wearable applications, the design and the fabrication of reconfigurable antennas, the characterization of antennas and microwave devices.

Mauro Mongiardo has received the laurea degree (110/110 cum laude) in Electronic Engineering from the University of Rome "La Sapienza" in 1983. In 1991 he has became associate Professor of Electromagnetic Fields and from 2001 he is full Professor of Electromagnetic Fields at the University of Perugia. He has been elected Fellow of the IEEE for "for contributions to the modal analysis of complex electromagnetic structures" in 2011.

The scientific interests of Mauro Mongiardo have concerned primarily the numerical modeling of electromagnetic wave propagation both in closed and open structures. His research interests have involved CAD and optimization of microwave components and antennas.

Mauro Mongiardo has served in the Technical Program Committee of the IEEE International Microwave Symposium from 1992. From 1994 he is member of the Editorial Board of the IEEE TRANSACTIONS ON MICROWAVE THEORY AND TECHNIQUES. During the years 2008-2010 he has been associate editor of the IEEE TRANSACTIONS ON MICROWAVE THEORY AND TECHNIQUES. He is author or co-author of over 200 papers and articles in the fields of microwave components, microwave CAD and antennas. He is the co-author of the books "Open Electromagnetic Waveguides" (IEE, 1997), and "Electromagnetic Field Computation by Network Methods" (Springer, 2009).

Luciano Tarricone received the Laurea degree in electronic engineering (cum laude) and Ph.D. degree from Rome University "La Sapienza," Rome, Italy, in 1989 and 1994, respectively. From 1990 to 1992, he was a Researcher with the IBM Rome Scientific Centers. From 1992 to 1994, he was with the IBM European Center for Scientific and Engineering Computing, Rome, Italy. Between 1994 and 1998, he was a Researcher with the University of Perugia, Perugia, Italy, and, between 1998 and 2001, he was a "Professore Incaricato" of electromagnetic (EM) fields and EM compatibility. Since November 2001, he has been a Faculty Member with the Department of Innovation Engineering, University of Salento, Lecce, Italy, where he is Full Professor of EM fields and coordinates a research group of about 15 people. He has authored and coauthored approximately 300 scientific papers. His main contributions are in the modeling of microscopic interactions of EM fields and biosystems, and in numerical methods for efficient CAD of microwave circuits and antennas. He is currently involved in bioelectromagnetics, electromagnetic energy harvesting and wireless power transmission, novel CAD tools and procedures for microwave circuits, RFID, and EM high-performance computing.